Validation of a method for the determination of the sensible-heat flux with Sodar data in free convection cases (*)

S. FIACCONI ([1]), M. I. PENDESINI ([2]), C. CASSARDO ([3]) and G. FRUSTACI ([1])

([1]) *Centro Meteorologico Regionale, Servizio Meteorologico dell'Aeronautica - Milano, Italy*
([2]) *Dipartimento di Fisica, Università di Milano - Milano, Italy*
([3]) *Dipartimento di Scienze e Tecnologie Avanzate, Università di Alessandria - Alessandria, Italy*

(ricevuto il 5 Febbraio 1996; revisionato il 14 Febbraio 1997; approvato il 24 Marzo 1997)

Summary. — A simple method to determine the value of the ground sensible-heat flux using Sodar data is presented and validated. The measurement of the variance of the wind velocity components gives us an estimate of the intensity of the atmospheric turbulence; the local value of variance of the vertical wind velocity σ_w^2 depends on the efficiency of thermal and mechanical turbulence production. The portion of the atmospheric boundary layer, where turbulent kinetic energy is prevalently produced by buoyancy forces, is characterised by profiles of σ_w^3/z and of (sensible-) heat flux which decrease linearly with height. The extrapolation to the ground of the former profile gives an estimate of the value of sensible-heat flux at the surface. The validation of the results is performed by comparison of the energy involved in the development of convective episodes calculated, over the same time interval, from sensible-heat flux at the surface with that derived from potential temperature profiles relative to two successive radio soundings. When perturbative processes like, for example, rise up of breezes, are absent, the estimates of energies are in excellent agreement, being the angular coefficient of regression line 1.01 and the linear correlation coefficient 0.93.

PACS 92.60 – Meteorology.

1. – Introduction

The PBL (planetary boundary layer) shows a typical daily evolution in high-pressure conditions. The diurnal change of the PBL characteristics is due to the solar radiation input that, heating the soil surface, triggers the convective motions which, starting from the lower levels, create the so-called mixed layer. The significant scaling parameters for the description of the diurnal PBL are the height of the mixed layer, z_i, and momentum and heat fluxes at the ground. During the night, due to long-wave counter radiation, the Earth gets colder, thus promoting the development of a stable layer characterised by an inversion of temperature. The growth of the inversion height in the Po Valley is given by the relationship $z = 70\sqrt{t}$ [1], where z is given in meters above the surface and t in hours after sunset.

(*) The authors of this paper have agreed to not receive the proofs for correction.

In this paper, we describe a method that, beginning from the measurements of the vertical velocity variance obtained from the Sodar, allows us to estimate the sensible heat flux (SHF) at the ground: results are shown and validated, and limits to the applicability of the method are discussed.

The importance of the SHF can be easily understood if we note that the available atmospheric energy, which is the cause of all atmospheric motions, is given in a indirect way by the Sun. The absorption of the solar radiation from the atmosphere is in fact negligible; indeed, the heating of the atmosphere derives from exchange processes at the surface in form of latent (Q_E) and sensible (Q_H) heat fluxes. The relative importance of the two fluxes depends on the ground humidity and on the type of surface (canopy and/or soil composition), and is expressed by the Bowen ratio

$$\beta = \frac{Q_H}{Q_E} = \frac{c_p}{L_v} \frac{\overline{w' \theta'_s}}{\overline{w' q'_s}}, \tag{1}$$

where w', θ' and q' are fluctuations of vertical velocity, potential temperature and specific humidity, respectively, and the index "s" indicates the values at the surface; c_p is the specific heat at constant pressure for the dry air and L_v the latent heat of evaporation/condensation. This ratio is small (≈ 0.2) on moist terrain, where the greater part of the energy coming from the Sun is spent in the process of evaporation, and it is greater in the driest regions (≈ 5 in semiarid regions; [2]).

The SHF is responsible for the heating of the air during sunny days, while the contribution of latent-heat flux is valuable only in condensation processes. The determination of the SHF value appears fundamental in weather and climate forecast models; once its value at the ground is known, its extrapolation to the top of the PBL will constitute the initial datum for numerical models. In the same way, the estimate of surface SHF is fundamental in models of pollutant dispersion as it is an indicator of the degree of stability of the atmosphere. Besides, it appears in many similarity relationships regarding significative variables of the mixed layer: for example, the value of $\overline{w' \theta'_v}$ allows us to estimate the value of the temperature structure parameter C_T^2, which can also be derived from Sodar measurements, and even of the mixed layer height z_i when this height overcomes the range of the instrument or is not evidenced by the characteristics of echo [3, 4]. Finally, SHF together with echo vertical profiles, on the basis of an original algorithm developed by the authors [4-6], can be used to calibrate the Sodar.

The interest in the SHF legitimates the efforts accomplished when defining measurement techniques and empirical relationships that allow its estimations. Among these, we could remember the method of eddy correlation that, taking into account the *Taylor hypothesis* [7], needs rapid response instruments for the measurement of the variables of interest, in this case w and θ_v. A further elaboration allows us to reconstruct the temporal series of the fluctuations w' and θ'_v from which $\overline{w' \theta'_v}$ (the SHF at the height at which the instrument set has been positioned) is drawn. The major disadvantage of this method arises from the necessity of arranging a complex instrumentation, easily subject to impairments, and large data storage systems to save the great quantity of collected data.

Furtherly, since 1960, many authors have been trying to estimate in several ways the value of σ_w, a very important parameter both for the study of the pollutant diffusion and for its impact on the energetic budget of the PBL [8]. An estimation of the SHF from Sodar data has been performed by different authors using similarity

relationships, including both measures of σ_w^3/z and of C_T^2 [9-12]; they denounce the tendency of Sodar to overestimate the lower values of SHF, due to the lack of convective conditions in the first hours of the day. But, generally speaking, the flux values obtained with different measurements techniques agree with those by Sodar, being differences generally lower than 10-20% [13].

2. – Sensible-heat flux and diurnal convection: Basic theory

The correlation existing among the trend in time of the solar radiation and the sensible- and latent-heat fluxes have brought to the introduction of simple empirical relationships [2, 14, 15] which parameterize the heat fluxes directly as a function of radiation. Such formulas, justified whenever the fluxes cannot be obtained in a different way, are quite correct only for averaged values, while instantaneous values could sometimes be not appropriate.

Other methods use theoretical formulas, like those proposed by Businger and Dyer [2, 14], in which the value of the ground flux depends on the values of the averaged variables; anyway these relations do not take into account modifications to vertical profiles due to phenomena which do not depend on the surface value of the flux [16]. In the same way, relations involving the ratio between fluxes of heat and momentum shift the problem to the evaluation of another turbulent quantity, $\overline{u'w'}$.

2˙1. *Relation between sensible-heat flux and* C_T^2. – The extremely regular trend of the Sodar echo profile during the diurnal hours (mainly near local noon) is well described by the formula of Wyngaard *et al.* [17], originally derived for the convective surface layer (SL) with the help of the similarity theory and subsequently extended to the mixed layer [18]:

$$\frac{C_T^2}{T^2} = \frac{4}{3(kg)^{2/3}} \left(\frac{\overline{w'\theta'_s}}{T} \right)^{4/3} z^{-4/3}, \tag{2}$$

where z is the height, g the gravity acceleration, k the Von Karman constant and T the absolute temperature. The dependence on $z^{-4/3}$ appears to be an intrinsic characteristic of the answer of the acoustic signal in a convective atmosphere [19]. On the other hand, the knowledge of the C_T^2 profile and $\overline{w'\theta'_s}$ flux at the ground permits us to evaluate the height of the mixed layer and vice versa [20, 21].

In order to evaluate the SHF in a well-mixed layer, and to extrapolate its value to the ground, we use the variance of the vertical velocity measured by the Doppler Sodar. In 1960, the hypothesis of Panofsky and McCormick [22] assumed that the variance of the vertical wind velocity σ_w^2 at a certain height depends on the height, z, and on the local rate at which the kinetic turbulent energy increases.

2˙2. TKE *equation*. – The equation of the average turbulent kinetic energy (TKE) has the following form:

$$\frac{\partial \bar{e}}{\partial t} + \overline{U_j} \frac{\partial \bar{e}}{\partial x_j} = \delta_{i3} \frac{g}{\bar{\theta}_v} (\overline{u_i' \theta_v'}) - \overline{u_i' u_j'} \frac{\partial \overline{U_i}}{\partial x_j} - \frac{\partial (\overline{u_j' e})}{\partial x_j} - \frac{1}{\bar{\varrho}} \frac{\partial \overline{u_i' p'}}{\partial x_i} - \varepsilon , \tag{3}$$

I II III IV V VI VII

where $i, j = 1, 2, 3$ and the Einstein convention is used. The meaning of each term in eq. (3) is the following: term I is the local change of TKE; term II is the advection of TKE by mean wind; term III is its buoyant (thermal) production (or consumption), due to the heat flux $\overline{w'\theta'_v}$; term IV accounts for its mechanical production or consumption due to the wind shear; term V is the turbulent transport; term VI accounts for the redistribution of TKE by pressure perturbations; and finally term VII is the viscous dissipation.

The rate of molecular (viscous) dissipation ε is always positive: in fact the turbulence is dissipative and tends to decrease in time if it is not locally generated or transported by the wind, pressure fluctuations or other turbulent processes. The term ε is greater for the small-scale eddies: more intense is the turbulence at small scale, more efficient is the process of dissipation. Equation (3) could be simplified assuming a coordinate system aligned with the mean wind, horizontal homogeneity and neglecting subsidence. We obtain

$$\frac{\partial \bar{e}}{\partial t} = \frac{g}{\bar{\theta}_v}\overline{w'\theta'_v} - \overline{u'w'}\frac{\partial \bar{U}}{\partial z} - \frac{\partial(\overline{w'e'})}{\partial z} - \frac{1}{\varrho}\frac{\partial(\overline{w'p'})}{\partial z} - \varepsilon\,. \tag{4}$$

I III IV V VI VII

In convective situations the mechanical production of TKE (IV) is important in the lowest layers, where a positive wind shear and a negative momentum flux result in production of turbulence. This term cancels out in the mixed layer, where the wind tends to be constant. The buoyant production of turbulent kinetic energy (III) decreases linearly with height above the SL where it is almost exactly balanced by the dissipative term. The buoyancy force acts vertically so it contributes to the production of turbulence only along that direction. The term of turbulent transport (V) is responsible for the return to the isotropy of the turbulence itself. In the SL it is negative, while it becomes positive in the mixed layer, so there is a net transport of TKE toward the top. In absence of fluxes of turbulent energy at ground or at the top of the layer, the integral of $\partial(\overline{w'e'})/\partial z$ over all the layer is null, then the effect of this term is just a redistribution of the TKE. The term related to the pressure fluctuations (VI) is measurable with difficulty and usually is neglected in the budget.

At night, the atmosphere is stable: the production of turbulence is exclusively mechanical, and the contributions of the buoyancy forces and the transport terms are negligible. In these conditions, stationary, non-homogeneous, continuous turbulence can be influenced by the growth of atmospheric stability, and the governing scales of the classical non-local similarity theory could be no more representative [23].

2˙3. *Diurnal convective case.* – Following [22, 24], in which it is assumed that the vertical variance value depends on the height z and on the TKE local increasing rate, and considering that, in convective cases, the prevailing terms of TKE production in the budget equation are the mechanical ($\varepsilon_1 = \overline{u'w'}(\partial\bar{u}/\partial z)$) and thermal ones ($\varepsilon_2 = \overline{w'\theta'_v}(g/\theta_v)$), it is possible to do a dimensional analysis of the terms in eq. (4) and write

$$\sigma_w^2 = A[z(\varepsilon_1 + \delta\varepsilon_2)]^{2/3}, \tag{5}$$

where A and δ are "universal constants" [24]. In a dry convective layer, $\theta'_v \approx \theta'$; when the convective processes dominate, we should retain the mechanical production of

turbulence negligible, and eq. (5) could be furtherly simplified to:

$$\sigma_w^2 = \alpha \left(z \frac{g}{\overline{\theta}} \overline{w'\theta'} \right)^{2/3}, \tag{6}$$

where $\alpha = A\delta^{2/3}$. Such constant has been evaluated from Caughey and Readings [8] by means of a direct comparison at a fixed height among measures of σ_w and of fluxes; the value we chose (after the comparison with the results obtained by other authors) is that of Weill *et al.* [24]: $\alpha = 1.4$.

Equation (6) can be rewritten as

$$\frac{\sigma_w^3}{z} = \alpha^{3/2} \frac{g}{\overline{\theta}} \overline{w'\theta'}. \tag{7}$$

From this relation, it results that the value of the ratio σ_w^3/z is directly proportional to the SHF at the same height z, hence it is possible by means of a Doppler Sodar to reconstruct the vertical profile of this ratio and then to evaluate the flux values.

2˙4. *Surface flux of sensible heat.* – The equation of conservation of the thermal energy can be written as:

$$\underset{\text{I}}{\frac{\partial \overline{\theta}}{\partial t}} + \underset{\text{II}}{\overline{u}_j \frac{\partial \overline{\theta}}{\partial x_j}} = \underset{\text{III}}{-\frac{1}{\varrho c_p} \left[L_v E + \frac{\partial \overline{Q}_j^*}{\partial x_j} \right]} \underset{\text{IV}}{- \frac{\partial (\overline{u_j'\theta'})}{\partial x_j}}, \tag{8}$$

where Q_j^* is the net radiation component in the j-th direction, L_v the latent-heat flux of evaporation, c_p the specific heat for moist air at constant pressure, E the rate of phase change in evaporation and $\overline{u_j'\theta'}$ the turbulent heat flux in the j-th direction. Applying scale analysis, we obtain that the more relevant terms are:

$$\frac{\partial \overline{\theta}}{\partial t} + \overline{w} \frac{\partial \overline{\theta}}{\partial z} = - \frac{\partial \overline{w'\theta'}}{\partial z}. \tag{9}$$

Indeed, the contributions to the energy budget coming from the horizontal advection (term II in eq. (8)), from the radiation and latent heat flux, due to the processes of evaporation/condensation (term III) and from the horizontal divergence (term IV) are actually negligible. The hypotheses assumed for these simplifications are particularly valid if anticyclonic situations in the Po Valley are considered. The very low wind regime that characterizes these situations allows us to neglect the advective terms; divergence terms are not significant according to the hypotheses of horizontal homogeneity, and the residual terms are small if compared to the others.

In the mixed layer the temperature profile is adiabatic, then $\partial \overline{\theta}/\partial z = 0$ and we have observed that $\partial \overline{\theta}/\partial t = \text{const}$. This leads us to conclude that also $\partial \overline{w'\theta'}/\partial z = \text{const}$, *i.e.* the SHF decreases linearly with the height [24]. If we take eq. (7) again, we could replace the linear trend with the value of the SHF at the ground writing:

$$\frac{\sigma_w^3}{z} = \alpha^{3/2} \frac{g}{\overline{\theta}} \overline{w'\theta'_s} \left(1 - \frac{z}{h'} \right), \tag{10}$$

where h' represents the height at which, by linear interpolation, the flux becomes zero. We point out that the height h' does not coincide with the real height at which the value

of the flux is zero, even if it is close to it. We should remember that the fluxes in the mixed layer are positive but in the entrainment layer they change sign. In fact, air cells generated by convective motions rise up and bypass the top of the mixed layer, which is capped by a thermal inversion. The relatively warmer air in the inversion, for mass continuity, is forced to descend. The upward motion of the colder air and the downward motion of warmer air contribute to give a negative value to the SHF [2].

We conclude this section observing that relation (10) allows the determination of the value of kinematic SHF at the ground by extrapolation to $z = 0$ of the vertical profile of σ_w^3/z, that is actually linear with height in the mixed layer if the hypotheses at the basis of our theory are correct.

3. – The Sodar

The instrument used in this work is a Sensitron Sodar installed at Cameri (near Novara, in the Po Valley, North-West Italy, located 168 meters a.s.l.), next to the airport of the Italian Military Air Force. The Sodar Sensitron is a Doppler monostatic triaxial system. Three antennas are opportunely oriented and work in sequence. Each antenna operates in monostatic way emitting a short resounding monochrome impulse and then receiving the echoes backscattered by thermal turbulence elements. The antenna vertically oriented picks up and analyzes the echo in its components of amplitude and frequency, and takes information on the local fluctuations of temperature and on the magnitude of the vertical wind. The two lateral antennas just make the spectral analysis of the received signal, giving the components of the wind velocity along the direction of the axis of the antenna. The software of the instrument allows us to quickly obtain the real value of the three Cartesian wind components and their relative standard deviations. The transmitting and receiving sections of the apparatus are checked by a microprocessor system, while the analysis of the shift in frequency of the Doppler effect is performed by a PLL quartz circuit. The height at which the echo is originated is defined by the delay with which signals arrive at the microphone. The frequencies commonly used by Sodars are included within the interval 1–4 kHz: the best compromise among maximum range and minimum absorption and diffusion is achieved with a frequency around 2 kHz. At these frequencies, the instrument is sensible to the temperature and humidity fluctuations on distances of the order of 10–20 cm.

The Cameri Sensitron Sodar uses a frequency of 2300 Hz that, at the temperature of 15 °C, coincides to a wavelength of about 17 cm [25]. The noise at this frequency, being the instrument located in an rural area, is reduced to a minimum; the rare presence of marks not attributable to atmospheric motions is almost always recognizable on the layout facsimile.

The acoustic power P_R received by Sodar is given by the equation:

$$P_R = P_E \frac{AG}{z^2} \frac{c\tau}{2} \sigma e^{-2\alpha z} E_c, \tag{11}$$

where P_E is the emitted acoustic power, $c\tau/2$ the maximum depth of the effective scattering volume, c the sound velocity, τ the impulse duration, AG/z^2 the effective solid angle covered by the antenna cone at distance z, G the gain, $e^{-2\alpha z}$ the air attenuation factor during the wave travel, a the absorption coefficient, E_c the excess of attenuation [9] and finally σ the scattering.

4. – Selection of the experimental dataset

The dataset used for this work was collected at the Milan Regional Meteorological Center of the Italian Air Force Meteorological Service (hereafter referenced as CMR). In particular, we made use of the following data:

a) *Meteorological bulletins*

Issued daily by the National Center of Meteorology and Aeronautical Climatology (CNMCA) in Rome. They report: surface analysis and the meteorological map for southern Europe at 12.00 UTC of the previous day, lowest and highest temperatures of Italian and some European cities, surface and isobaric maps (500 hPa) and a detailed weather forecast for the current day.

b) METAR (*code messages*)

ICAO code messages containing hourly or semi-hourly observations, made in all Italian airports, of the following quantities: wind direction and intensity (in degrees and knots), horizontal visibility (in meters), contingent presence of distinctive phenomena near the ground like fog, hail or haze, type and degree of cloudy coverage (in eighths and cloud codes), height at which the clouds base is located (thousands of feet), temperature and dew point (in °C) and pressure (in hPa).

c) *Linate radiosoundings*

These data concern the radiosoundings performed with balloons four times a day at the principal synoptic hours (00.00, 06.00, 12.00, 18.00 UTC) at the Milan Airport (Linate, located 104 meters a.s.l.) and they comprise: height relative to the sea level (geopotential meters), pressure (hPa), temperature and dew point (°C), relative humidity (percent), mixing ratio (g/kg), wind direction and intensity (degrees and m/s); all these data are reported at the standard isobaric levels and at some significant points. We can remember that the starting time of each radiosounding is about one hour before its reference time (*i.e.* the radiosounding of 06.00 UTC starts at about 05.00 UTC). Because we are interested in the lower data of radiosoundings, this fact should be taken into account in the following considerations.

d) *Sodar data*

These are: echo amplitude (in arbitrary unity), quality indicator, horizontal wind speed (m/s), horizontal wind direction and its standard deviation, intensity and standard deviations of the three components of the wind (m/s). All data are given every 25 m of height along the vertical, echoes every 5 m. For details regarding the quality of the data used in measurements of this type, the reader is referred to [25, 26].

Once relationships between Sodar data and SHF have been focused, it is necessary to select meteorological situations in which our method can be applied. The data taken into account in our investigation were:

a) Sodar available soundings between the years 1990 and 1994. Before the quantitative analysis of the data, a selection using the quality indicator of the echo (that gives the number of echoes got from each height on which the software performs averages, relative to the 107 impulses dispatched in the half hour integration time) has been made. We eliminated the values of echo and wind characterized by a quality indicator inferior to 10.

b) A selection, from the meteorological bulletins, of anticyclonic synoptic situations; in order to do this, we took into consideration only days in which the mean sea level pressure on the Po Valley was not inferior to 1016 hPa.

c) A selection, from the METAR data of the Cameri station, of the cases with wind calm at the ground (velocity less than or equal to 2 knots) and absence of cloudiness.

Over the whole period, we considered 58 situations of high pressure: 30 are relative to the warmer months (April-September) and 28 to the colder months (October-March).

5. – Observations and results

The dataset consist of a series of records of the vertical velocity variance, measured every 25 m of height beginning from 50 m above the ground, obtained every half hour. The advised data concern only convective conditions and so they are limited to the sunshine hours, starting from around one hour after dawn, when the ground heating is sufficient to trigger convection.

In the morning the mixed layer grows slowly and achieves the maximum in the first hours of the afternoon; this process is evidenced by the growth of depth of the layer in

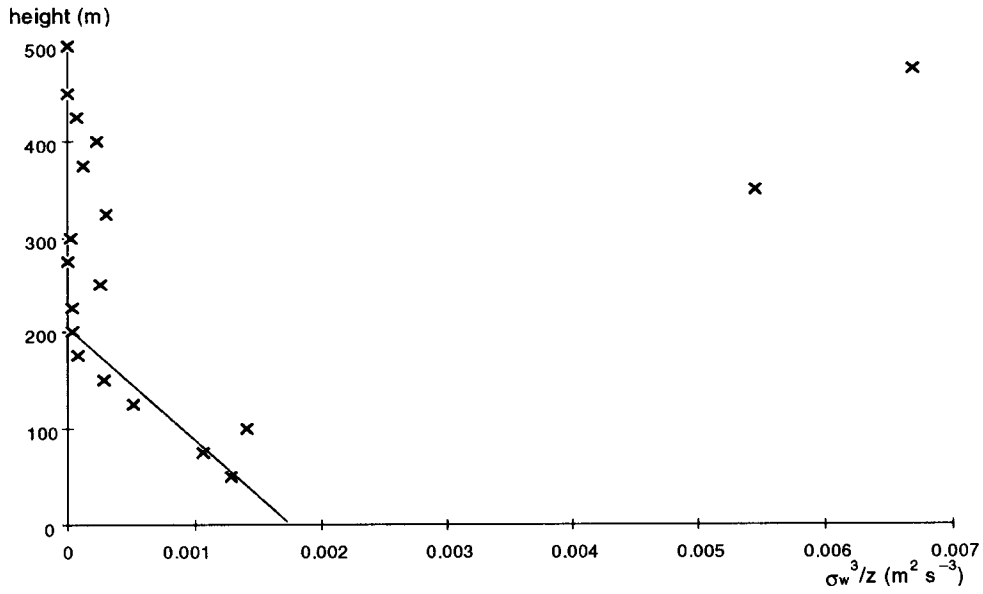

Fig. 1. – Vertical profile of σ_w^3/z relative to 5.50 UTC of July 19, 1992.

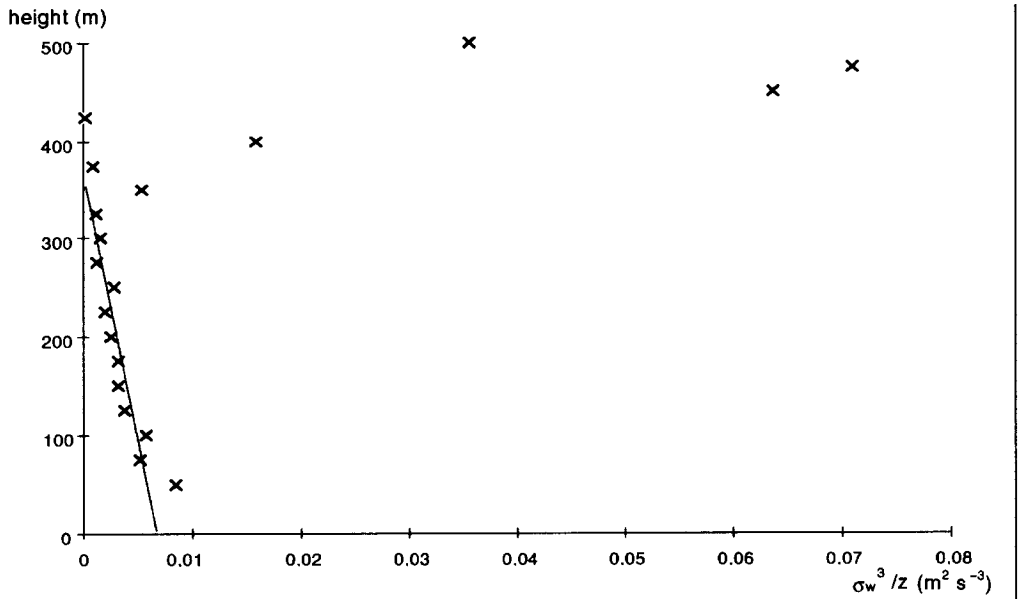

Fig. 2. – Vertical profile of σ_w^3/z relative to 10.50 UTC of July 19, 1992.

which the profile of σ_w^3/z is linear, as shown in the figs. 1 and 2. The linear behaviour is observed only in the lower part of the two profiles and its extension increases from 175 meters at 05.50 UTC to 325 meters at 10.50 UTC; the σ_w^3/z ratio is bigger in late forenoon than in the first morning due to the growth of convective motions and of heat fluxes with time as a consequence of the warming of the ground.

Frequently the linear decrease displayed by σ_w^3/z in the mixed layer is not observed in the lower layers, usually up to a height of about 100 m (fig. 3). This behaviour is not surprising if we consider that such levels are inside the SL, where mechanical production of TKE is not negligible. In fact, as can be seen in fig. 4, in the SL the intensity of the echo is very high. This is due to wind shear, which reach its maximum intensity near the surface. As the height increases, the echo decreases almost regularly: the values read in the Sodar file, in fact, already account for the effects of the intensity dump of sound wave (due both to the increase of the distance from the source, function of r^{-2}, and to the attenuation of sound wave into air [5, 6]).

Bearing these discussions in mind, and considering that the SL depth is about 10% of the PBL height, which in convective situations grows with time, we decided to exclude from the interpolation the lower four points, corresponding at least to a height of 125 m.

In the mixed layer, for low winds nearly constant with height, as frequently happens in high-pressure conditions, the turbulence generation by wind shear is negligible; this fact is confirmed by the linear trend of σ_w^3/z. A typical case is illustrated in figure 5: the intensity of the wind remains less than 2 m/s up to 300 m of height and increases slowly with altitude until the highest value of around 3 m/s at 475 m is reached; the σ_w^3/z profile (fig. 3) is very regular among 100 and 300 m, and the value of SHF obtained by extrapolating to zero this linear portion is 0.084 mK/s; this

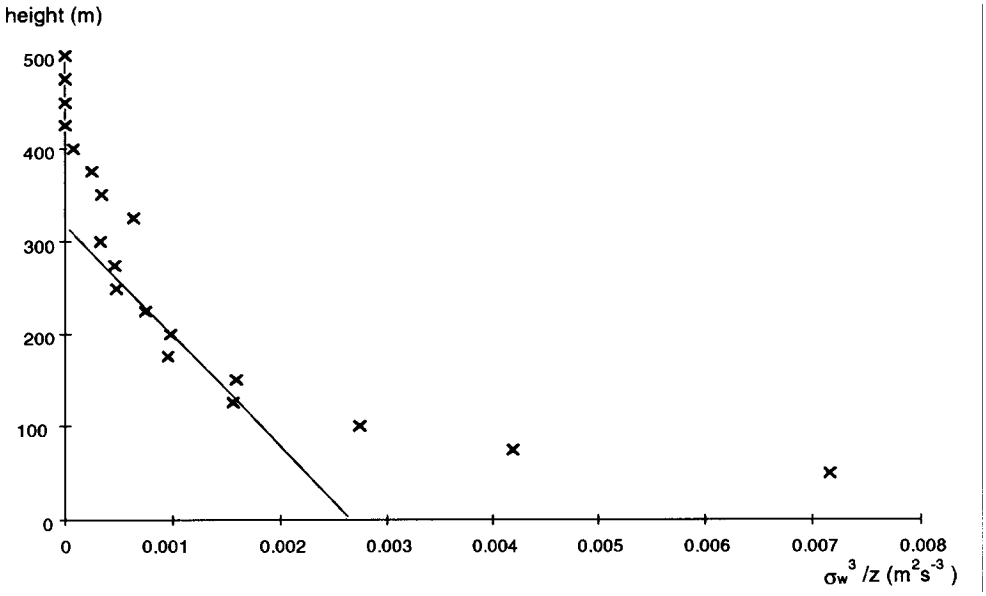

Fig. 3. – Vertical profile of σ_w^3/z relative to 9.20 UTC of October 10, 1990.

value is in good agreement with the evaluations obtained with the eddy correlation method in a typical morning of autumn in Po Valley [1, 26, 27]. The first three points which lie in the SL are evidently out of the linear trend of the higher levels, and have been neglected.

The situation shown in figs. 6, 7 is quite different: the local shear stress determines a large variation of σ_w^3/z and fluctuations of its value are observed also in the mixed layer where a linear trend of σ_w^3/z would be expected (fig. 6). In fact, the wind intensity, almost constant up to 250 m of height, changes abruptly at the upper levels (fig. 7). Therefore, the evaluation of SHF at the ground suggested by our method can not be applied: the anomalous course at the more elevated levels is a clear indication of the absence of the conditions in which the thermal convection is the dominant process of turbulence production. This turbulence structure has been frequently observed in the first afternoon of the summer months and is determined by the rise up of the breeze: such meteorological conditions constitute a limit to the application of the method.

We extracted from our Sodar file all cases displaying the linear course of σ_w^3/z. Subsequently this linear trend was extrapolated to the surface using a number of points varying from case to case; the average number of data used was ten, equivalent to an atmospheric layer of 250 m; however, we never made calculations using less than 6 values. The correlation coefficient for each linear fit was always elevated, with a mean value over all cases equal to 0.88.

At this point, for each selected anticyclonic situation, it is possible to infer the SHF at the ground beginning from about one hour after sunrise, using the profiles of σ_w^2 of the Sodar relative to conditions of calm and absence of cloudiness (free convection), previously verified on the basis of the METAR data. In this way, the time trend of the flux could be reconstructed at least up to the time in which the breeze, increasing its

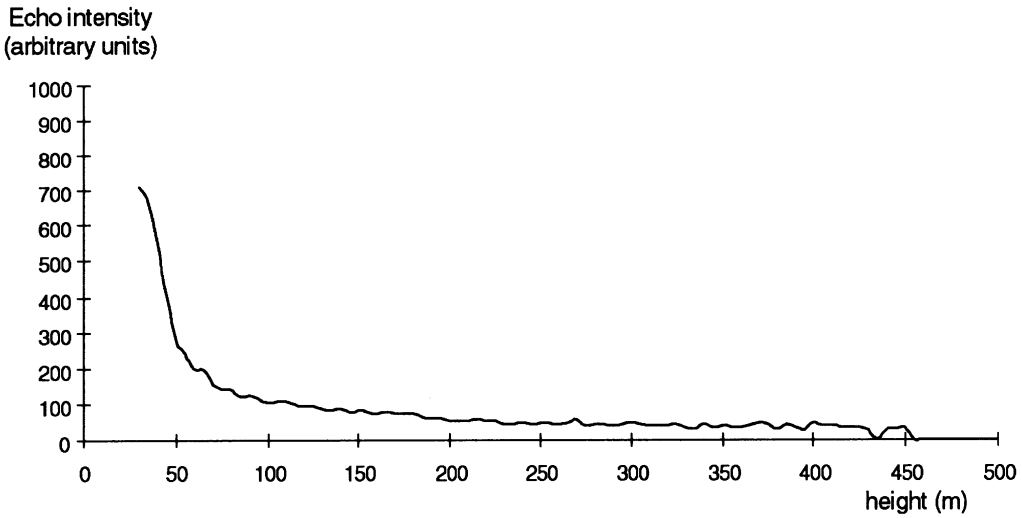

Fig. 4. – Vertical profile of echo intensity relative to 11.50 UTC of July 19, 1992.

intensity, alters the profile of σ_w^3/z in a significant way; in fig. 8 a typical example of the diurnal evolution of the kinematic SHF at ground, obtained with this method, is illustrated. The values we found are of the order of those found in the literature for the Po Valley [27].

The analysis of our results shows that, in general, the SHF reaches its maximum value about an hour after the culmination of sunshine (at 12.30 local time). However, we

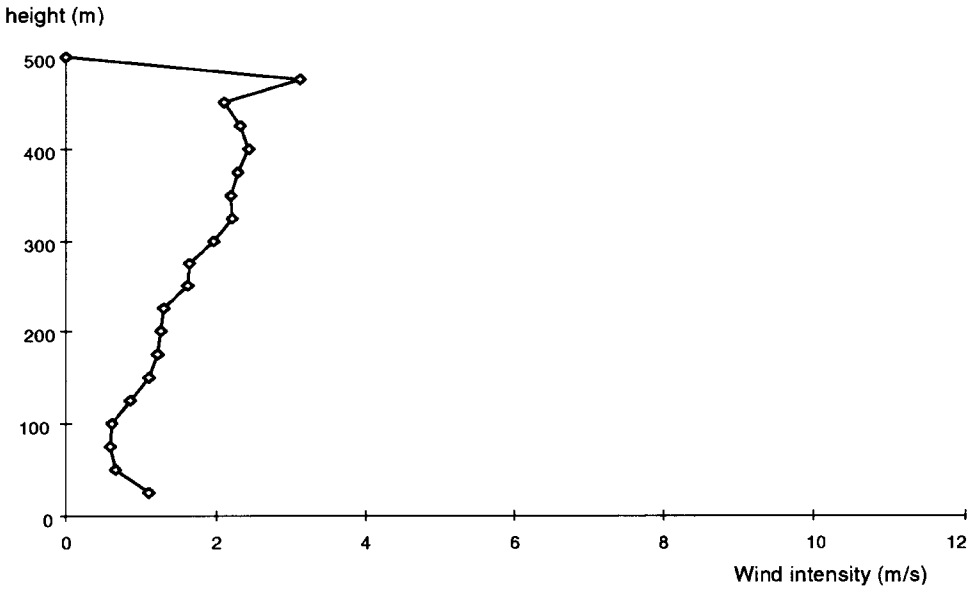

Fig. 5. – Vertical profile of wind intensity relative to 9.20 UTC of October 10, 1990.

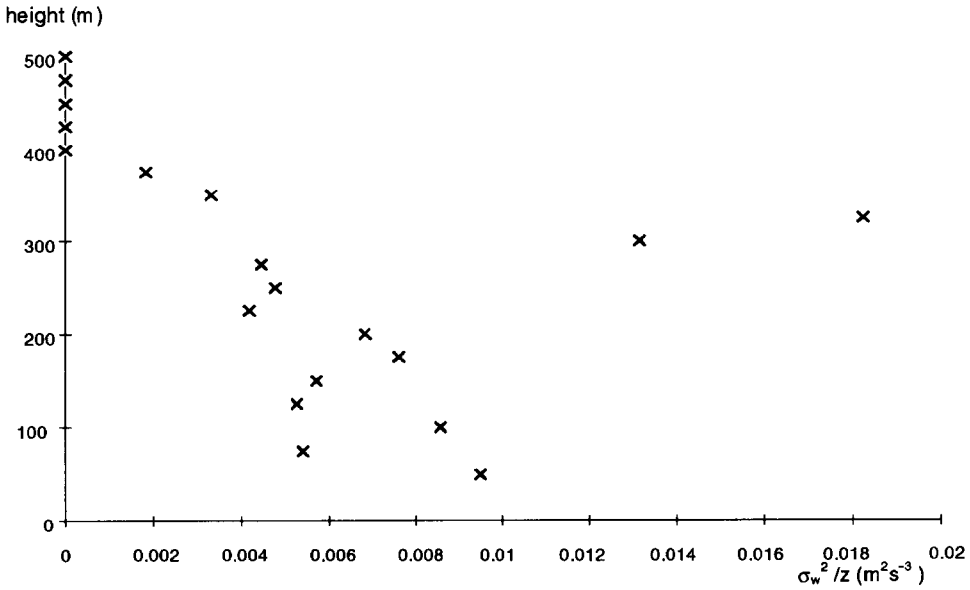

Fig. 6. – Vertical profile of σ_w^3/z relative to 14.20 UTC of July 15, 1992.

should remember that the individual flux values are subject to an error attributable partly to a temporary change of the atmospheric conditions that could lead to an increase of the mechanical production of turbulence, partly to the error with which the Sodar measures the variance of the vertical velocity, and finally to the intrinsic chaotic nature of the turbulent motions.

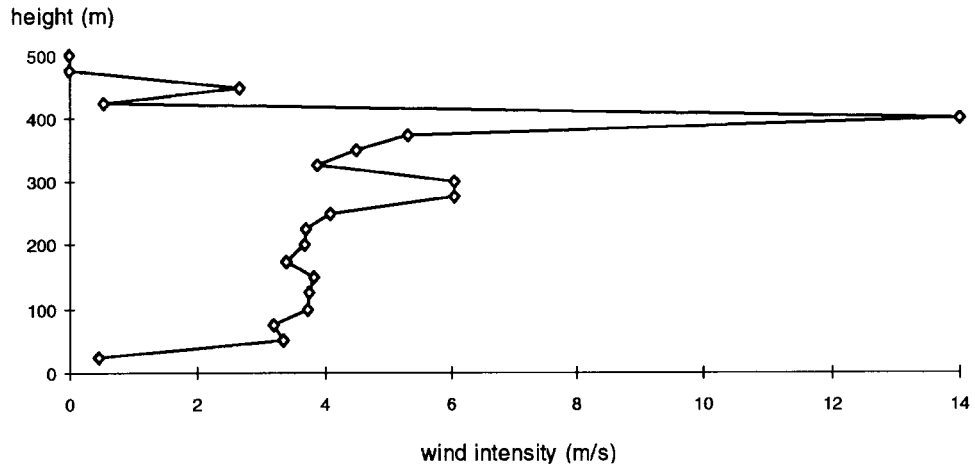

Fig. 7. – Vertical profile of wind intensity relative to 14.20 UTC of July 15, 1992.

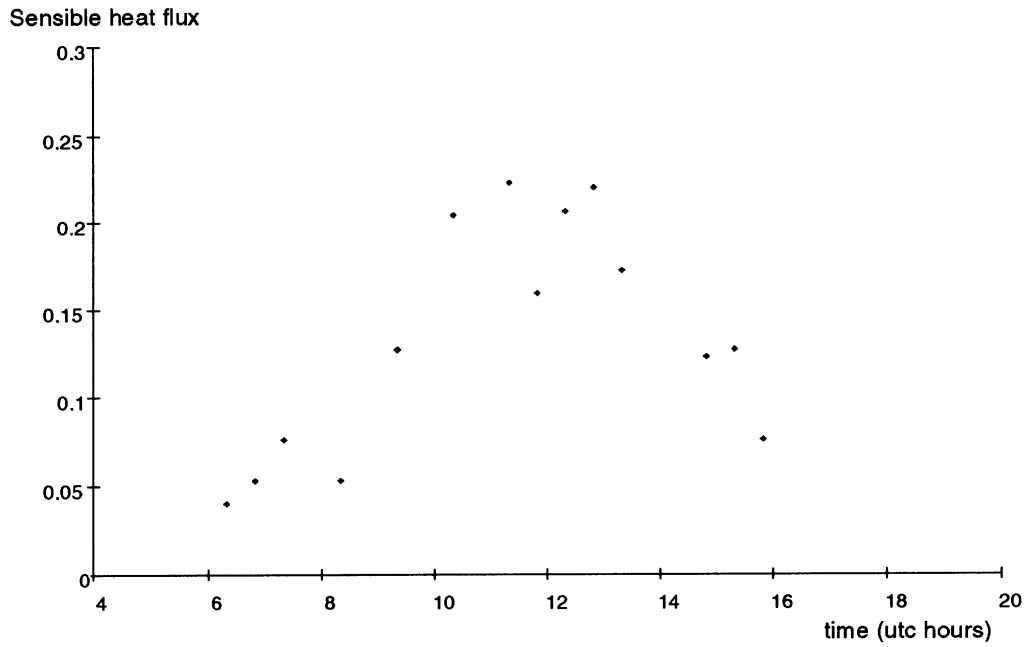

Fig. 8. – Time trend of sensible-heat flux relative to July 18, 1992.

6. – Verification of the sensible-heat flux evaluation

It is important to perform a validation of SHF evaluated applying the method previously described. From the Sodar data we get only measurements of σ_w^2 but we do not possess any alternative instrumentation to check the (goodness and) validity of our results. On the other hand, a direct comparison is not always decisive [9, 11, 28, 29]; with this technique we do not obtain an effective punctual value, as happens using rapid response instruments, but a datum that reflects the Sodar averages on a certain air volume. Besides, we must remember that unfortunately we do not have any way to evaluate directly, with a different kind of measurements, the precision with which the Sodar achieves the σ_w^2 values.

An indirect way to validate our method should be a comparison among the area covered by the diurnal evolution of the SHF and the corresponding one delimited by the two vertical profiles of the potential temperature reconstructed from the radiosoundings performed in Linate at 06.00 and 12.00 UTC time. The capability to compare measures gathered in two different sites, *i.e.* Linate as regards the radiosoundings and Cameri for the Sodar data, is supported by the homogeneity hypothesis that characterizes the Po Valley in high-pressure conditions (see appendix A). The two areas represent in different ways estimates of the energy involved in the development of convective events over the same time interval. In the first case this energy is calculated on the basis of half hour averages of SHF towards the atmosphere derived from Sodar data, while in the second it is expressed as a function of the heat exchange at the surface required to account for the variation of potential temperature profile within the mixed layer.

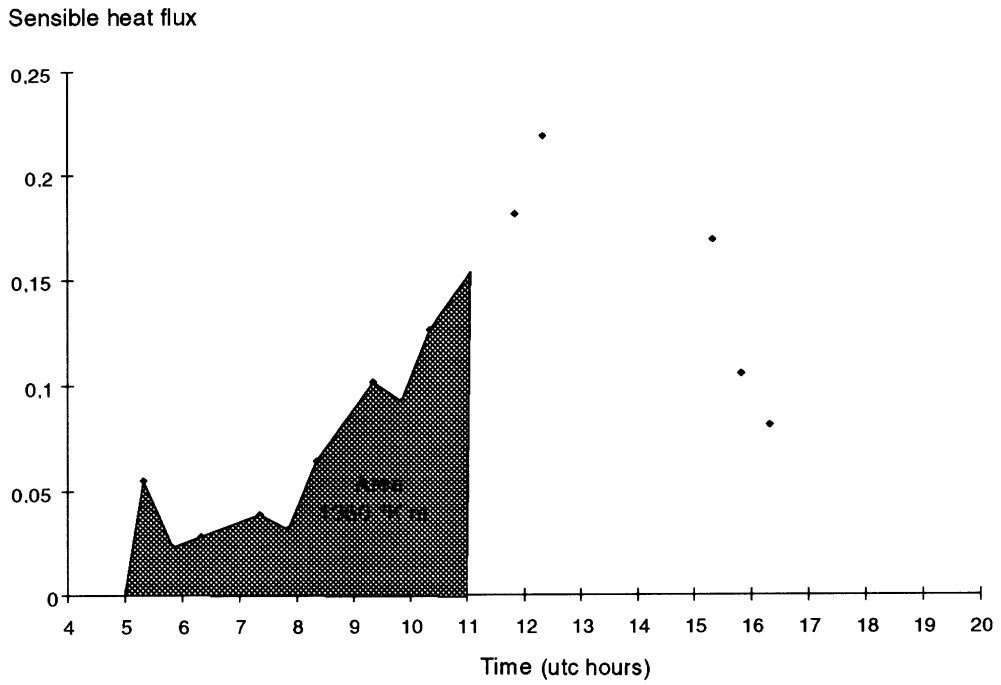

Fig. 9. – Area (in energetic units) covered by the curve of sensible-heat flux limited to 5.00 and 11.00 UTC of August 26, 1992.

Conditions of high pressure, low humidity and absence of clouds relative to the analyzed situations guarantee that air heating due to the release of latent heat by the condensation processes is negligible, while the dominant process of energy transfer is that driven by the SHF. The area included between radiosoundings carried out at 6.00 and 12.00 UTC represents the effective heating of the air; generally, the distance between two curves reduces with height. Regarding the flux, when it proved impossible to determine its value in correspondence to the morning radiosounding, a linear trend was supposed in order to connect it to the first available datum.

Figures 9 and 10 show an example of the comparison performed for one of the typical anticyclonic situations we examined; the SHF are evaluated between 5 and 11 UTC for the reason explained in subsect. **4** c); the area highlighted on the second picture is limited by the two radiosoundings of 06.00 and 12.00 UTC.

We selected and analyzed 36 situations taken from our database. Out of these, 8 were eliminated as unsuitable for the application of the method. In three cases all the necessary data to estimate the area delimited by the radiosoundings were not available; all the others concerned winter situations in which the stable anticyclonic condition gave origin to the formation of radiative fogs or to a ground-based inversion layer even during the day, so the required characteristic of convection is not fulfilled. The remaining data were divided into two groups relative to physically different cases. In the first one, the area from the radiosoundings prevails with respect to that measured with the fluxes: in all these situations the two potential temperature profiles continue to remain separated one from the other even at highest levels. When these

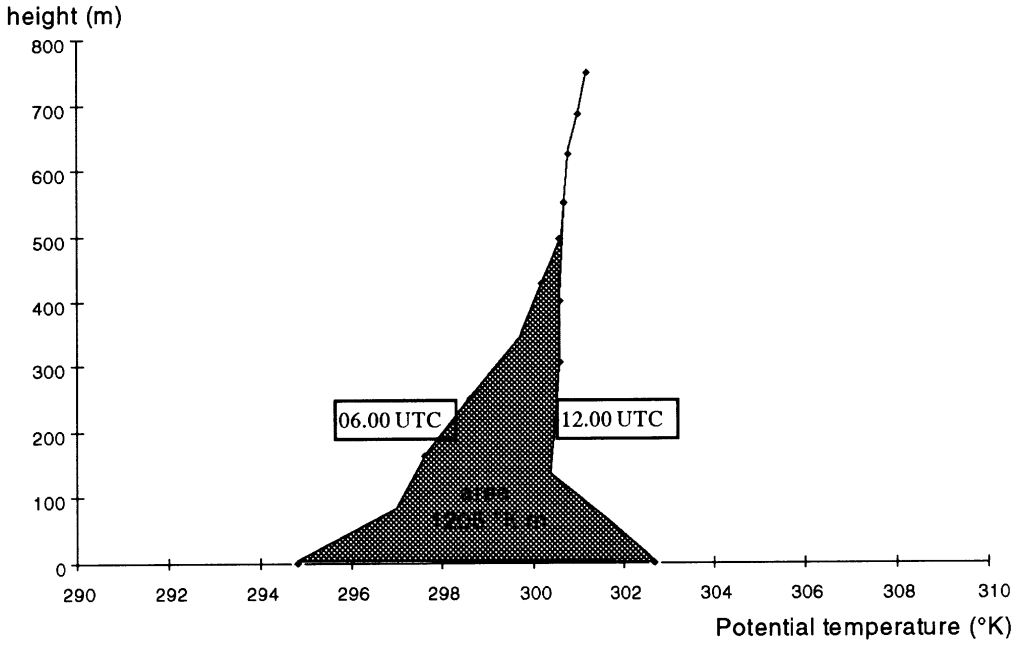

Fig. 10. – Area (in energetic units) included between the potential temperature profiles at 6.00 and 12.00 UTC of August 26, 1992.

conditions are met, we chose to calculate the area up to the top of the mixed layer, z_i, evaluated on the radiosounding of 12.00 UTC; the overestimation obtained in these cases could be ascribed to processes different from the ones we are taking into account, *i.e.* advection of warm air at upper levels. In the second group, the energy given from the SHF prevails: all these cases refer to a period (during summer 1993) in which the 06.00 UTC radiosoundings were not performed; in order to do the comparison, we used the temperature profiles measured at 00.00 UTC; but at that time the atmosphere has not completely cooled yet, then the area included between the potential temperature profiles of 00.00 and 12.00 UTC should underestimate the energy absorbed during the day.

After the elimination from our database of the points that belong to the two aforementioned groups, we obtained the results shown in fig. 11. The angular coefficient of the straight line calculated on 17 points is equal to 1.01 while the linear correlation coefficient is 0.93. The agreement between the two estimates of energy is good and confirms the initial hypothesis, that Sodar data allow the determination of the ground SHF, which is an important scaling parameter in the PBL. The closer the atmospheric conditions are to those in which the thermal convective turbulence prevails, the more this method proves to be applicable.

7. – Conclusions

In convective conditions, we applied an easy method that, starting from the values of the variance of the vertical wind velocity measured with a Sodar, calculates the SHF

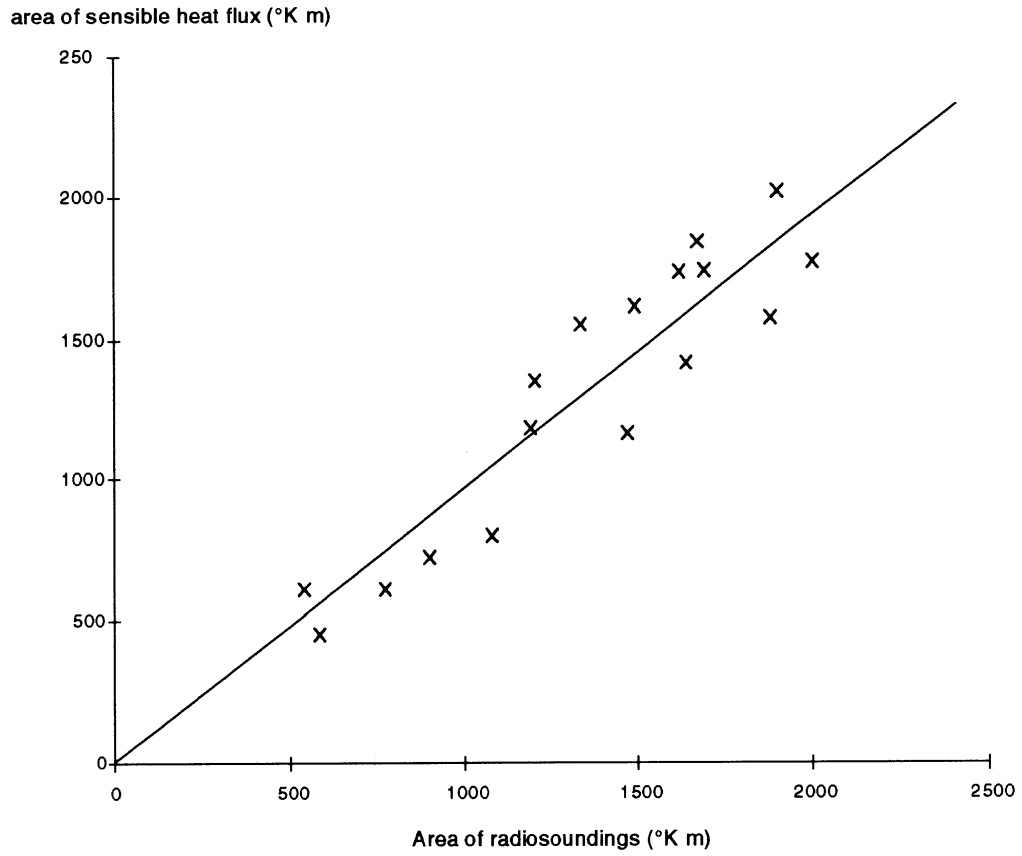

Fig. 11. – Comparison between the areas included by the sensible-heat flux trend and the vertical profiles of potential temperature in the time interval 06.00-12.00 UTC.

at ground, just extrapolating the linear part of the vertical profile of σ_w^3/z. The capability of the proposed method has been validated by comparing the estimation of SHF (energy transferred from soil surface to air) with the energy spent at the surface to heat the air itself, evaluated from the evolution of the potential temperature vertical profile between two radiosoundings. The results allow us to confirm the validity of the physical hypotheses on which this method is based.

The possibility to extend this method to less restrictive conditions and the comparison with the fluxes evaluated by using eddy correlation techniques (for instance the data provided by sonic anemometers) should be investigated in a future work.

* * *

We are grateful to Prof. A. LONGHETTO of the Dipartimento di Fisica Generale, Università di Torino, for the suggestions regarding the general outlines of this work.

APPENDIX A

The hypothesis of homogeneity

The use of data, for the comparison of the obtained results or the verification of the proposed methods, coming from two different sites, about 100 km apart, requires a hypothesis of homogeneity of the ABL over a sufficiently wide area of the Po Valley. Due to the alpine orographic barrier, in high-pressure conditions, the lower atmospheric layers of the Po Valley are often uncoupled with the large-scale circulation. The unique ways of access for air masses are through the Adriatic Sea and the Dinaric Alps, or around and across the low Ligurian Apennines. As the Po Valley is often out of the trajectories usually outlined by the low- and high-pressure centers, the baric changes are normally not high, even though they depend on the change of the conditions of the air masses [30].

Climatologic studies, performed by examining averaged monthly insulation, lowest and highest temperatures, days with precipitation or fog and their persistence, days characterised by thermal inversions over a period of 20 years among 1959 and 1979, pointed out the actual homogeneity of the west zone of the Po Valley as a region less involved in the influence of the Adriatic sea [31]. In anticyclonic, stable, conditions, such characteristics of homogeneity are more evident in the regime of particularly weak wind.

An easy verification of the real homogeneity of the meteorological conditions for the examined situations was effected comparing the typical daily trend of the temperatures, measured at screen level, at Cameri and Milan Linate averaged on 27 summer days characterised by anticyclonic conditions (fig. 12); during daytime, the two curves show the same changes in the compared values, even if there is an average difference of about 2-3 °C, due perhaps to the different height above sea level of the two stations (respectively, 168 and 104 m a.s.l.), while the surface characteristics of the two stations are quite similar. During the night, the temperature difference is larger, due probably to the heat island effect of Milan city.

The result of this comparison allows us to assume that the diurnal sunshine is the same in the two sites and causes a similar daily warming.

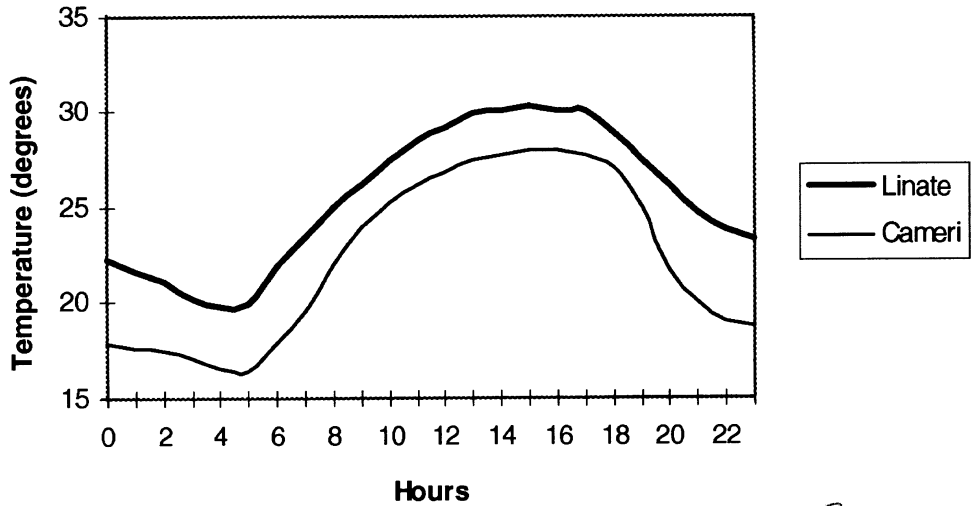

Fig. 12. – Comparison between the time evolution of the air screen temperature of Cameri (thin line) and Milan Linate (thick line) stations averaged on 27 summer days characterised by anticyclonic conditions.

REFERENCES

[1] ANFOSSI D., BACCI P. and LONGHETTO A., *Atmos. Environ.*, **8** (1974) 537.
[2] STULL R. B., *An Introduction to Boundary Layer Meteorology* (Kluwer Academic Publishers, Dordrecht) 1988.
[3] FIACCONI S., PENDESINI M. I., CASSARDO C. and FRUSTACI G., *Similarity parameters evaluation in Po Valley during convective situations by use of Sodar data, Nuovo Cimento C*, **19** (1996) 455.
[4] PENDESINI M. I., *Metodi di impiego del sondaggio acustico e loro applicazione in situazioni anticicloniche*, Degree thesis, Milan University, Italy (1994).
[5] FIACCONI S., PENDESINI M. I., CASSARDO C. and FRUSTACI G., *Validazione di un metodo per l'autocalibrazione del Sodar*, to be published in *Il Bollettino Geofisico* (1996).
[6] FIACCONI S., FRUSTACI G. and PENDESINI M. I., *Riv. Meteorol. Aeron.*, **LV** (1995) 31.
[7] TAYLOR G. I., *Proc. R. Soc. London, Ser. A*, **164** (1938) 476.
[8] CAUGHEY S. J. and READINGS C. J., *Adv. Geophys. A*, **18** (1975) 125.
[9] COULTER R. L. and WESELY M. L., *J. Appl. Meteorol.*, **19** (1980) 1209.
[10] KEDER J., FOKEN T. H., GERSTMANN W. and SCHINDLER V., *Boundary-Layer Meteorol.*, **46** (1989) 195.
[11] MELAS D., *Atmos. Environ.*, **24** (1990) 2847.
[12] MELAS D., *Boundary-Layer Meteorol.*, **57** (1991) 275.
[13] GREENHUT G. K. and MASTRANTONIO G., *J. Appl. Meteorol.*, **28** (1989) 99.
[14] DYER A. J., *Boundary-Layer Meteorol.*, **7** (1974) 363.
[15] ANFOSSI D., *Giornale di Fisica*, **1** (1982) 1.
[16] DE BRUIN H. A. R., KOHSIEK W. and VAN DEN HURK B. J. J. M., *Boundary-Layer Meteorol.*, **63** (1993) 231.
[17] WYNGAARD J. C., IZUMI Y. and COLLINS S. A. jr., *J. Opt. Soc. Am.*, **61** (1971) 1646.
[18] WYNGAARD J. C. and LEMONE M. A., *J. Atmos. Sci.*, **37** (1980) 1573.
[19] ASIMAKOPOULOS D. N., COLE R. S. and VAUGHAN O. O., *Boundary-Layer Meteorol.*, **10** (1976) 137.
[20] BEYRICH F., *Atmos. Environ. A*, **26** (1992) 2459.
[21] HILL R. J., OCHS G. R. and WILSON J. J., *J. Atmos. Ocean. Technol.*, **9** (1992) 526.
[22] PANOFSKY H. A. and MC CORMICK R. A., *Q. J. R. Meteorol. Soc.*, **86** (1960) 495.
[23] LONGHETTO A., ZHOU L. Y., BONINO G., CASSARDO C., GIRAUD C. and RICHIARDONE R., *Nuovo Cimento C*, **17** (1994) 579.
[24] WEILL A., KLAPSIZ C., STRAUSS B., BAUDIN F., JAUPART C., VAN GRUNDERBEECK and GOUTORBE J. P., *J. Appl. Meteorol.*, **80** (1980) 199.
[25] FAGGIAN P., *Caratterizzazione dello strato di confine planetario mediante sondaggio acustico*, Degree thesis, Milan University, Italy (1990).
[26] FAGGIAN P., FIACCONI S. and VECCIA E., *Riv. Meteorol. Aeron.*, **LII** (1992) 47.
[27] GIULIACCI M., *Riv. Meteorol. Aeron.*, **XLI** (1981) 153.
[28] NEFF W. D. and COULTER R. L., *Acoustic Remote Sensing in Probing the Atmospheric Boundary Layer* (AMS, Boston, Mass.) 1986.
[29] THOMAS P. and VOGT S., *Boundary-Layer Meteorol.*, **15** (1978) 375.
[30] BORGHI S. and GIULIACCI M., *Nuovo Cimento C*, **34** (1980) 1.
[31] GIULIACCI M., *Climatologia statica e dinamica della Valpadana* (CNR, Milan, Italy) 1985.